

AN ADVANCED COMPRESSION OPTION FOR THE EUROPEAN XFEL

I. Zagorodnov, M. Dohlus, E.A. Schneidmiller, M.V. Yurkov
 Deutsches Elektronen-Synchrotron, Hamburg, Germany

Abstract

An advanced compression scheme which allows to obtain a high peak current while preserving the low slice emittance is considered. The beam is compressed weakly in the bunch compressors and the current is increased by ESASE setup at the entrance of the undulator line. It is shown by numerical studies that such approach allows to reduce harmful collective effects in the bunch compressors and in the transport line. Simulations of FEL physics confirm the possibility to obtain a high level of SASE radiation at the ultra-hard photon energy level of 100 keV.

INTRODUCTION

The European XFEL provides SASE photon beams for user operation since 2017 [1]. Currently it has three photon lines (SASE1, SASE2, SASE3, see Fig. 1) and should reach the photon energy of 25 keV [2].

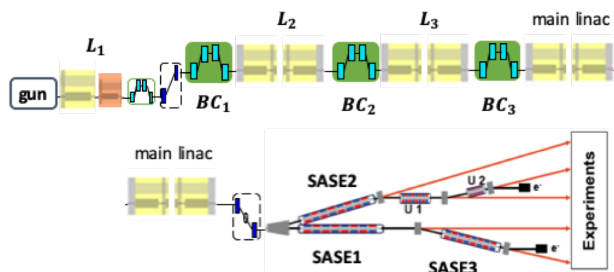


Figure 1: The European XFEL layout.

There is a possibility to use one of free tunnels (U1 or U2, see Fig. 1) for the ultrahard x-ray undulator line to produce the SASE photons with energy of 100 keV [3]. We study two possible scenarios: standard compression to 5 kA and an advanced compression with ESASE setup [4] up to 10 kA. The latter compression scheme allows to reduce the collective effects and to obtain a better electron slice parameters and to reach a higher level of SASE energy per electron bunch.

ACCELERATOR BEAM DYNAMICS

We have done numerical modeling of the accelerator beam dynamics up to the entrance of SASE2 undulator line. We have not included the effect of the last arc from SASE2 to U1 tunnel. The electron bunch with charge of 100 pC has been compressed to 2 and 5 kA. In the choice of the working points we have followed the approach of paper [5] and have used two codes: Ocelot [6] and Krack3 [7].

The tracking of particles in Ocelot is done in the same way as, for example, in Elegant [8]. Quadrupoles, dipoles, sextupoles, RF cavities and other lattice elements are modeled by linear and second order maps. The focusing effect of RF cavities is taken into account according to the

Rosenzweig-Serafini model. The space charge forces are calculated by solving the three-dimensional Poisson equation in the bunch frame. The CSR module uses a fast ‘projected’ one-dimensional method [9]. The wakefields and the incoherent synchrotron radiation (ISR) effects are included.

Beam Dynamics in Linac

Table 1: Compression Parameters

| Parameter | 5 kA | 2 kA |
|-------------------------------|------------------|------|
| energies $E_1/E_2/E_3$, MeV | 130 / 700 / 2400 | |
| R_{56}^1/R_{56}^2 , mm | 56 / 52 | |
| compression factors C_1/C_2 | 3.5 / 28 | |
| R_{56}^3 , mm | 55 | 37 |
| total compression C_3 | 862 | 340 |
| Z'_3 , 1/m | | 0 |
| Z''_3 , 1/m/m | 600 | 300 |

In standard operation we compress the electron bunch to the peak current of 5 kA and accelerate it to 17.5 GeV. The parameters of the longitudinal beam dynamics are listed in Table 1. The positive value of the second derivative of the inverse compression function Z_3 allows to reduce the compression strength in the bunch head [5]. To suppress the microbunching instability the energy spread in the bunch was increased in the laser heater, which is installed before the injector dogleg. The power of the laser is chosen to have at the linac end the rms slice energy spread of 1 MeV. The results of the simulation are shown in Fig. 2. The bunch has relatively small slice emittance: 0.2 μm in the horizontal plane and 0.3 μm in the vertical plane. The projected emittances are listed in Fig. 2 as well. The larger slice emittance in the y-plane is due to CSR effects in the vertically oriented bunch compressors. The larger horizontal projected emittance and the ‘‘banana’’ shape of the bunch in x-plane are due to not compensated CSR effects in the switchyard arc before SASE2 undulator line.

In order to suppress the self-fields and to improve the bunch properties we consider another compression scenario: to compress the same bunch to 2 kA current in the linac and to 10 kA current in ESASE setup in the vicinity of the undulator line. The main parameters are listed in Table 1. The power of the heater is chosen to have after main linac the rms slice energy spread of 0.65 MeV. The results of the simulation for the bunch before ESASE setup are shown in Fig. 3. The bunch has slice emittance of 0.2 μm in both planes. The projected emittances in both planes are by factor 2 smaller than in the former case. Nevertheless, we see a larger projected emittance in the horizontal plane due to CSR impact in the arc before SASE2 undulator line.

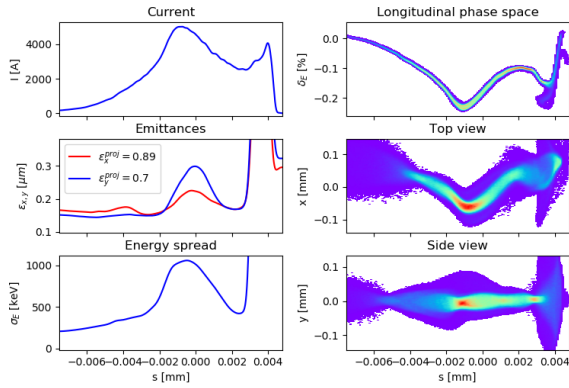


Figure 2: Electron beam properties at SASE2 entrance for the beam compressed to 5 kA.

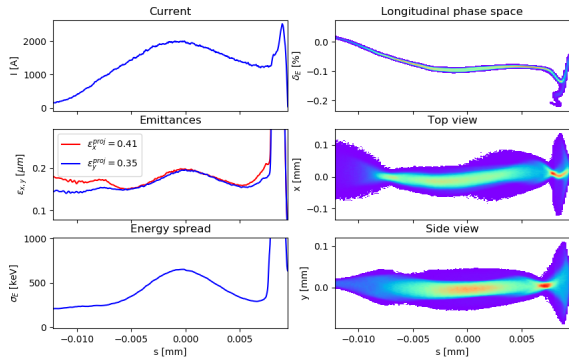


Figure 3: Electron beam properties at SASE2 entrance for the beam compressed to 2 kA.

Beam Dynamics in ESASE Setup

Table 2: ESASE Setup Parameters

| Parameter | |
|----------------------------------|------|
| modulator period λ_w , m | 0.7 |
| chicane magnet field strength, T | 0.25 |
| chicane magnet length, m | 1 |
| chicane parameter R_{56} , mm | 0.78 |
| laser power P_L , GW | 8 |
| laser spot size w_0 , mm | 0.65 |

Figure 4 shows the layout and the optics of ESASE setup. The main parameters of the setup are listed in Table 2. The bunch from Fig. 3 is tracked with Ocelot taking into account the incoherent and the coherent synchrotron radiation effects.

The electron beam passes two periods of the wiggler with period λ_w of 0.7 m. At the same time a laser pulse with wave length λ of 800 nm propagates through the wiggler collinearly with the electrons and impose energy modulations. The wiggler parameter K is equal to 73.2 and the maximal deviation of the reference electron from the orbit $r_{max} = K/(\gamma k_w)$ is 0.24 mm. The transverse rms beam size is equal to 25 μm . Hence, taking into account r_{max} , we choose the laser spot size to be 0.65 mm. It gives the

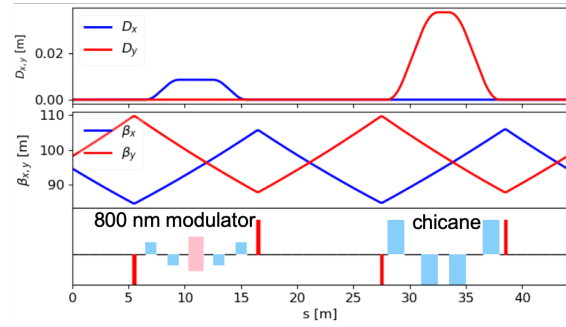


Figure 4: Layout and optics of ESASE setup.

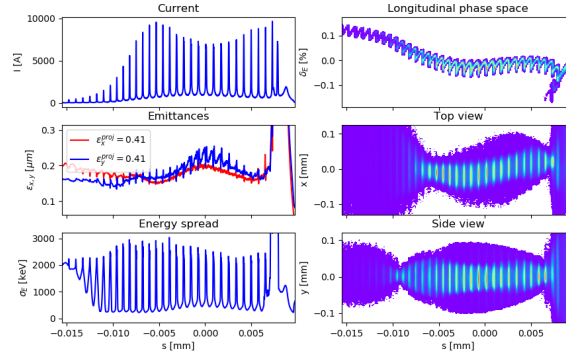


Figure 5: Electron beam properties after ESASE setup.

relatively large Rayleigh length of 1.7 m which is larger than the wiggler length L_w of 1.4 m.

The amplitude of the energy change in the wiggler can be found as

$$\Delta E = \sqrt{\frac{P_L}{P_A} \frac{2KL_w mc^2}{\gamma w_0}} \left(J_0 \left(\frac{K^2}{4 + 2K^2} \right) - J_1 \left(\frac{K^2}{4 + 2K^2} \right) \right),$$

where $\gamma = E_b/(mc^2)$, $P_A = I_A mc^2/e$, I_A is Alfven current. The laser pulse has a peak power P_L of 8 GW, which gives the energy modulation amplitude ΔE equal to 3.14 MeV.

Next the electron beam passes through the dispersive magnetic chicane. In order to produce the maximal microbunching the chicane parameter R_{56} has to be chosen near to the value $R_{56}^0 = E_b/(\Delta E k)$ which is equal to 0.7 mm. To compensate the effect of self-fields it is adjusted to 0.78 mm.

After the chicane we have enhancement of the electron peak current and the slice energy spread by approximately factor $C = \Delta E/\sigma_E$ which in this case is equal to 4.8.

Figure 5 shows the electron beam parameters after ESASE setup. We see the enhancement of the current from 2 kA to 10 kA. Simultaneously the energy spread at the position of the current spikes increases to 3 MeV. The slice and the projected emittances in the deflection plane of the chicane increase slightly due to CSR impact.

RADIATION PROPERTIES AT 100 keV

The technology of in-vacuum undulators is well developed and used at other facilities. We consider SASE4 undulator with undulator period of 22 mm and the active length of

175 m. The SASE4 undulator could be installed in U1 tunnel (see Fig. 1). For the time being in our analysis we consider SASE2 tunnel. This position takes into account the impact of the switchyard arc.

The simulations are done with three-dimensional code ALICE [10] for the photon energy of 100 keV. We have used the real number of the electrons and have included the energy losses and quantum fluctuations due to synchrotron radiation in the undulator. To compensate the energy loss and to increase the energy in the photon pulses we have used a non-linear taper for the rms undulator parameter:

$$K = K_0 - 1.5 \cdot 10^{-5} z[m] - 1.3 \cdot 10^{-6} (z[m] - 90)^2 H(z[m] - 90),$$

where $K_0 = 0.567393$ and $H(\cdot)$ is the Heaviside function.

The left plot in Fig. 6 shows the energy in the photon pulse along the SASE4 undulator beam line. The red solid line corresponds to the bunch with the peak current of 5 kA shown in Fig. 2. At the end of the undulator line it reaches the SASE energy of 40 μ J. The SASE power along the pulse for one shot is shown in red on the right plot in Fig. 6. The lasing part is relatively narrow due to the optics and the orbit mismatch along the electron bunch.

The blue solid line on the left plot in Fig. 6 corresponds to the bunch after ESASE setup with the peak current of 10 kA shown in Fig. 5. At the end of the undulator line it reaches the SASE energy of 110 μ J. The SASE power along the pulse for one shot is shown in blue in Fig. 7. Due to the transverse shifts of the slices seen in Fig. 5 we have not managed to bring all current spikes to the same level of lasing power.

To estimate the impact of the synchrotron radiation in the switchyard arc to SASE2 undulator we have additionally considered the case when SASE4 undulator has the position in the SASE1 tunnel (see Fig. 1). The corresponding results are shown by dashed curves on the left plot in Fig. 6. The beam with the peak current of 5 kA produces the photon pulses with energy of 50 μ J. It is only small increase compared to the former case for SASE2 tunnel. The beam with the peak current of 10 kA, formed by ESASE setup, produces the photon pulses with total energy of 180 μ J. It gives factor 2 difference to the former case for SASE2 tunnel.

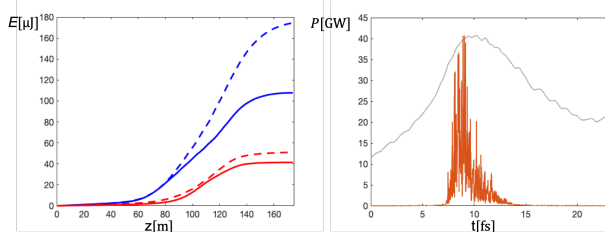


Figure 6: The left plot shows the SASE energy along SASE4 undulator. The red curves presents the results for nominal compression to 5 kA. The blue curves show the results for eSASE setup. The solid lines present the results for SASE2 tunnel. The dashed lines show the results for SASE1 tunnel. The right plot presents the SASE power for the 5kA beam in SASE2 tunnel.

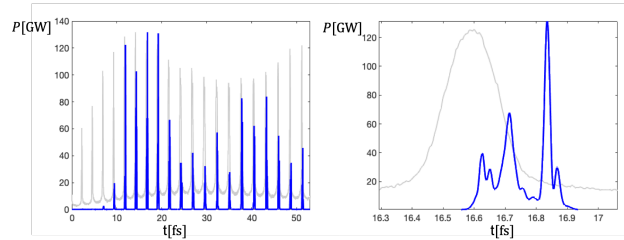


Figure 7: Photon power with eSASE setup for SASE2 tunnel. The gray curves show the current profile.

MICROBUNCHING AND CSR ISSUES

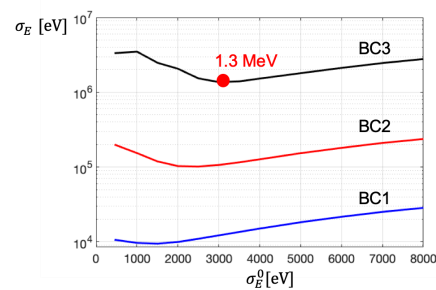


Figure 8: The slice energy spread due to microbunching for the bunch with the peak current of 2 kA vs. the initial energy spread after the laser heater.

In the simulations presented above we have been optimistic and took quite small values for the final slice energy spread. In the simulations we have used $5 \cdot 10^6$ macroparticles and could not resolve the parasitic microbunching effects in the linac. For this reason we have done a devoted study of the minimal energy spread after the linac for the case when we take into account the microbunching due to the space charge forces. In our study we have used the periodic Poisson solver [11] and the real number of electrons in the slice. We have varied initial energy σ_E^0 at the position of the laser heater and have analyzed the energy spread after the bunch compressors. The results for the charge of 100 pC compressed to the peak current of 2 kA are shown in Fig. 8. We see that the estimation of the minimal slice energy spread is equal to 1.3 MeV. It is two times larger as the energy spread of 0.65 MeV used in the simulations of the previous sections. For the beam with the peak current of 5 kA our estimation is even more pessimistic. With the current optics and the compression scenario we will have more than 4.5 MeV of the slice energy spread [12]. We are looking now for possible solutions to reduce the microbunching.

The analytical estimation gives 0.2 MeV slice energy spread from the ISR. However, the impact of the CSR on the bunch properties is considerable. As it can be seen from Fig. 6 we need to suppress the CSR effects in the switchyard arc to SASE2 and are looking now for possible solutions as well [13, 14].

REFERENCES

- [1] H. Weise and W. Decking, “Commissioning and First Lasing of the European XFEL”, in *Proc. FEL’17*, Santa Fe, NM, USA, Aug. 2017, pp. 9–13. doi:10.18429/JACoW-FEL2017-MOC03
- [2] E.A. Schneidmiller and M.V. Yurkov, “Photon beam properties at the European XFEL”, DESY Report No. DESY 11-152, XFEL.EU TR-2011-006, 2011.
- [3] E. Schneidmiller *et al.*, “Considerations for the Ultrahard X-ray Undulator Line of the European XFEL”, in *Proc. IPAC’19*, Melbourne, Australia, May 2019, pp. 1732–1735. doi:10.18429/JACoW-IPAC2019-TUPRB023
- [4] A.A. Zholents, “Method of an enhanced self-amplified spontaneous emission for x-ray free electron lasers”, *Phys. Rev. ST Accel. Beams*, vol. 8, pp. 040701, 2005. doi:10.1103/PhysRevSTAB.8.040701
- [5] I. Zagorodnov, M. Dohlus, and S. Tomin, “Accelerator beam dynamics at the European X-ray Free Electron Laser”, *Phys. Rev. Accel. Beams*, vol. 22, pp. 024401, 2019. doi:10.1103/PhysRevAccelBeams.22.024401
- [6] S. I. Tomin, I. V. Agapov, M. Dohlus, and I. Zagorodnov, “OCELOT as a Framework for Beam Dynamics Simulations of X-Ray Sources”, in *Proc. IPAC’17*, Copenhagen, Denmark, May 2017, pp. 2642–2645. doi:10.18429/JACoW-IPAC2017-WEPAB031
- [7] M. Dohlus, *Krack 3 User Guide*, DESY, 2018.
- [8] M. Borland, *User’s Manual for Elegant*, APS-ANL, Chicago, IL, 2017.
- [9] E.L. Saldin, E.A. Schneidmiller, and M.V. Yurkov, “Radiative interaction of electrons in a bunch moving in an undulator”, *Nucl. Instrum. Methods Phys. Res. A*, vol. 417, no. 1, pp. 158-168, 1998. doi:10.1016/S0168-9002(98)00623-8
- [10] I. Zagorodnov, “Numerical Modeling of Collective Effects in Free Electron Laser”, in *Proc. ICAP’12*, Rostock-Warnemunde, Germany, Aug. 2012, paper TUAC11, pp. 81–85.
- [11] M. Dohlus and Ch. Henning, “Periodic Poisson model for beam dynamics simulation”, *Phys. Rev. Accel. Beams*, vol. 19, pp. 034401, 2016. doi:10.1103/PhysRevAccelBeams.19.034401
- [12] M. Dohlus, “3D simulation of microbunching due to space charge effects”, talk at S2E meeting, DESY, 2019. www.desy.de/fel-beam/s2e/talks.html#a2019.04.16
- [13] S. Di Mitri *et al.*, “Cancellation of Coherent Synchrotron Radiation Kicks with Optics Balance”, *Phys. Rev. Lett.* vol. 110, pp. 014801, 2013. doi:10.1103/PhysRevLett.110.014801
- [14] T. Hara *et al.*, “High peak current operation of x-ray free-electron laser multiple beam lines by suppressing coherent synchrotron radiation effects”, *Phys. Rev. Accel. Beams*, vol. 21, pp. 040701, 2018. doi:10.1103/PhysRevAccelBeams.21.040701